Title

Lin28a Regulates Pathological Cardiac Hypertrophic Growth Through Pck2-Mediated Enhancement of Anabolic Synthesis

Journal

Circulation, 139(14)

ISSN

0009-7322

Authors

Ma, Hong

Yu, Shuo

Liu, Xiaojing

et al.

Publication Date

2019-04-02

DOI

10.1161/circulationaha.118.037803

Circulation

ORIGINAL RESEARCH ARTICLE

Lin28a Regulates Pathological Cardiac Hypertrophic Growth Through Pck2-Mediated Enhancement of Anabolic Synthesis

Hong Ma, MD, PhD
Shuo Yu, MD
Xiaojing Liu, PhD
Yingao Zhang, BS
Thomas Fakadej, BS
Ziqing Liu, PhD
Chaoying Yin, PhD
Weining Shen, PhD
Jason W. Locasale, PhD
Joan M. Taylor, PhD
Li Qian, PhD
Jiandong Liu, PhD

BACKGROUND: Hypertrophic response to pathological stimuli is a complex biological process that involves transcriptional and epigenetic regulation of the cardiac transcriptome. Although previous studies have implicated transcriptional factors and signaling molecules in pathological hypertrophy, the role of RNA-binding protein in this process has received little attention.

METHODS: Here we used transverse aortic constriction and in vitro cardiac hypertrophy models to characterize the role of an evolutionary conserved RNA-binding protein Lin28a in pathological cardiac hypertrophy. Next-generation sequencing, RNA immunoprecipitation, and gene expression analyses were applied to identify the downstream targets of Lin28a. Epistatic analysis, metabolic assays, and flux analysis were further used to characterize the effects of Lin28a and its downstream mediator in cardiomyocyte hypertrophic growth and metabolic remodeling.

RESULTS: Cardiac-specific deletion of *Lin28a* attenuated pressure overload–induced hypertrophic growth, cardiac dysfunction, and alterations in cardiac transcriptome. Mechanistically, Lin28a directly bound to mitochondrial phosphoenolpyruvate carboxykinase 2 (*Pck2*) mRNA and increased its transcript level. Increasing *Pck2* was sufficient to promote hypertrophic growth similar to that caused by increasing Lin28a, whereas knocking down *Pck2* attenuated norepinephrine-induced cardiac hypertrophy. Epistatic analysis demonstrated that Pck2 mediated, at least in part, the role of Lin28a in cardiac hypertrophic growth. Furthermore, metabolomic analyses highlighted the role for Lin28a and Pck2 in promoting cardiac biosynthesis required for cell growth.

CONCLUSIONS: Our study demonstrates that Lin28a promotes pathological cardiac hypertrophy and glycolytic reprograming, at least in part, by binding to and stabilizing *Pck2* mRNA.

Key Words: cardiac hypertrophy ■ glycolysis ■ Lin28a ■ metabolism ■ Pck2

Sources of Funding, see page 1739

https://www.ahajournals.org/journal/circ

ORIGINAL RESEARCH ARTICLE

Clinical Perspective

What Is New?

- The highly conserved RNA-binding protein, Lin28a, plays a critical role in pathological cardiac hypertrophy.
- Lin28a directly binds to mitochondrial phosphoenolpyruvate carboxykinase 2 (*Pck2*) mRNA to increase its transcript level and enhance cardiomyocyte biosynthesis during hypertrophic growth.
- Pck2 mediates, at least in part, the role of Lin28a in cardiac hypertrophic growth and glycolytic reprogramming.

What Are the Clinical Implications?

- The identification of Lin28a as a new regulator of pathological cardiac hypertrophy adds RNA posttranscriptional regulation as a new regulatory mechanism underlying pathological cardiac hypertrophy.
- Lin28a/Pck2-mediated metabolic repatterning during the early stage of cardiac hypertrophy is instrumental in cardiac structural remodeling, providing a potential therapeutic target for pathological cardiac hypertrophy.

Cardiac hypertrophy is often associated with diverse pathological conditions such as mechanical overload, hypertension, and ischemic injury.[1,2] Although the hypertrophic mechanism has been generally regarded as compensatory in conferring resistance to cardiac stress, prolonged growth predisposes individuals to intractable heart failure and sudden cardiac death. As such, recent basic and preclinical studies suggest that the attenuation of pathological hypertrophy has a beneficial effect of mitigating the development of heart failure,[1,3] making it a promising target for therapeutic interventions. Although significant advances in the treatment of pathological hypertrophy have been achieved, the commonly prescribed medications for pathological hypertrophy, including angiotensin-converting enzyme inhibitors, angiotensin receptor blockers, β-receptor blockers, calcium channel blockers, and others, usually bring about regression of left ventricular mass by 10% to 20% in human patients,[4] an in-depth knowledge of the molecular basis of this detrimental process could have considerable impact for the development of more potent therapeutics.[4,5]

When subjected to pathological stimuli, the heart undergoes extensive metabolic and structural changes characterized by a switch from fatty acid oxidation to greater reliance on glycolysis and hypertrophic growth of the cardiomyocytes, respectively.[6] The hypertrophic heart also demonstrates enhanced flux of metabolic intermediates into biosynthesis. Although the effect of metabolic remodeling on cell growth and proliferation has been increasingly recognized, questions remain on whether and how the metabolic remodeling during pathological hypertrophy contributes to myocardial hypertrophic growth, and the molecular regulation of this metabolic remodeling, as well.

The extensive cardiac structural and metabolic changes during pathological hypertrophy involve profound global alterations in cardiac transcriptome.[7] In addition to transcriptional regulation of cardiac gene expression,[8] RNA-binding protein–mediated posttranscriptional regulation has emerged as a critical layer for the control of gene function during health and diseases.[9,10] The RNA-binding proteins bind to diverse RNAs and intimately influence every aspect of RNAs' metabolism throughout their lifecycle, including biogenesis, stability, splicing, cellular localization, and translation.[10,11] Through inhibition of microRNA *let-7* maturation or directly binding to mRNAs to regulate their abundance and translation, the evolutionarily conserved RNA-binding protein Lin28a and its paralogue Lin28b play critical roles in pluripotency, organismal growth, tissue repair, and oncogenesis.[12,13] Much of these diverse functions of Lin28 have been attributed to its role in regulating cellular metabolism, yet the exact mechanisms differ depending on the biological contexts, highlighting the complexity of Lin28-mediated metabolic regulation. For instance, in the context of whole-animal physiology, Lin28 modulates glucose metabolism through regulating mechanistic target of rapamycin signaling in a *let-7*–dependent manner.[14] In contrast, during tissue repair, Lin28 enhances glycolysis and oxidative phosphorylation independently of *let-7* by directly binding to and enhancing the translation of the mRNAs of multiple rate-limiting enzymes involved in the glycolysis and oxidative phosphorylation.[15] A recent study on oncogenesis further demonstrates an important role of Lin28 in promoting aerobic glycolysis in cancer cells via targeting pyruvate dehydrogenase kinase 1.[16] Despite the important role of Lin28 in metabolic regulation, it remains to be explored whether Lin28 may regulate cardiac metabolism during pathological hypertrophy, and how exactly this regulation contributes to pathological structural remodeling.

In this study, we revealed a critical role of Lin28a in pathological cardiac hypertrophy and metabolic repatterning. Cardiac-specific deletion of *Lin28a* blunted pressure overload–induced cardiac hypertrophy and suppressed cardiac fibrosis. This effect of *Lin28a* on cardiac pathological hypertrophy likely occurred in a *let-7*–independent manner. Through RNA deep sequencing, bioinformatics analyses, and RNA immunoprecipitation assay, we identified *Pck2,* which encodes the mitochondrial phosphoenolpyruvate carboxykinase, as a direct target of Lin28a in cardiomyocytes. Lin28a directly bound to *Pck2* mRNA and positively impacted its

expression level. It is remarkable that, whereas knockdown of *Pck2* partially suppressed Lin28a-induced cardiomyocyte hypertrophic growth, overexpressing *Pck2* reversed the attenuation of norepinephrine-induced hypertrophy by loss of *Lin28a* function. Furthermore, metabolomic analyses indicated that the Lin28a/Pck2 axis promoted the cardiac biosynthesis required for cell growth. Our study thus demonstrates that Lin28a promotes pathological cardiac hypertrophy through regulating biosynthesis.

METHODS

The data, analytic methods, and study materials will be made available to other researchers for purposes of reproducing the results or replicating the procedure on reasonable request. The detailed methods are provided in the online-only Data Supplement.

Animals

All experiments involving animals were performed in accordance with the University of North Carolina at Chapel Hill Institutional Animal Care and Use Committee (IACUC) approved protocols.

Statistical Analysis

All data were presented as mean±SEM and statistically analyzed using SPSS or Prism software. The 2-tailed independent sample *t* test was used to compare the mean difference between 2 groups. One-way or 2-way ANOVA was used to compare the mean from ≥3 groups. If ANOVA analysis showed significant difference, then the Least Significant Difference test or the Tukey multiple comparison test was applied for post hoc analysis to detect the pairwise difference while adjusting for multiplicity. $P<0.05$ was considered statistically significant.

RESULTS

Upregulation of *Lin28a* by Mechanical and Neurohumoral Stimuli

Previous studies demonstrated that *Lin28a* responds to cellular stress[17] and promotes tissue repair.[15] We thus postulate that *Lin28a* may play a role in cardiac remodeling under stress conditions. To test this hypothesis, we first determined if *Lin28a* responded to mechanical stress. We analyzed *Lin28a* expression in a mouse model of cardiac hypertrophy whereby the transverse aorta was constricted to induce pressure overload. Unlike its paralogue *Lin28b, Lin28a* was barely detectable in sham-operated control mouse hearts, yet its expression was rapidly induced at both transcript and protein levels in the adult hearts after transverse aortic constriction (TAC) with the protein expression reaching its peak level at 3 days after TAC surgery (Figure 1A and 1B, Figure IA and IB in the online-only Data Supplement, and Table I in the online-only Data Supplement). We also found that the response of *Lin28a* to TAC surgery was similar, albeit slightly delayed, to that of the early-response genes such as *c-Jun* and *c-Myc* (Figure IA in the online-only Data Supplement and Table I in the online-only Data Supplement), suggesting that Lin28a might act downstream of the early-response genes.[18,19] In parallel, we assessed the response of *Lin28a* expression to neurohormonal agonists. Likewise, *Lin28a*, but not *Lin28b*, was significantly upregulated in isolated neonatal rat cardiomyocytes (NRCMs) in response to angiotensin II or norepinephrine (NE; Figure 1C).

Lin28a Plays a Significant Role in NE-Induced Cardiac Hypertrophy

As a first step to test the requirement for *Lin28a* in stress-induced cardiac hypertrophy, we assessed the effect of manipulating *Lin28* expression on NE-induced NRCM hypertrophy. Whereas NRCMs infected with nontargeting small interfering RNA (siRNA) control (si*NT*) developed massive hypertrophy after *NE* treatment, the NE-induced NRCM enlargement was markedly suppressed by siRNAs against *Lin28a* (si*Lin28a*; Figure 1D through 1F and Figure IC in the online-only Data Supplement). si*Lin28a* consistently suppressed NE-induced upregulation of hypertrophic markers atrial natriuretic peptide (*Anp*) and brain natriuretic peptide (*Bnp*; Figure 1G and 1H). Conversely, lentiviral-mediated *Lin28a* overexpression (Lenti-*Lin28a*) caused a substantial increase in the size of NRCMs in comparison with lentiviral control (Lenti-*Con*; Figure 1I and 1J and Figure ID in the online-only Data Supplement), and upregulated the expression of *Anp* and *Bnp* (Figure 1K and 1L). It is more important that lentiviral-mediated *Lin28a* overexpression in adult mouse hearts also upregulated the expression of fetal genes such as *Anp*, *Bnp*, α-skeletal muscle actin (*Acta1*), and myosin heavy chain beta (*Myh7*), and led to an increase in cardiomyocyte size (Figure IE through IG in the online-only Data Supplement and Table I in the online-only Data Supplement, and data not shown).

Loss of Cardiac *Lin28a* Blunted Pressure Overload–Induced Cardiac Hypertrophy

Next, we sought to determine the functional involvement of *Lin28a* in stress-induced cardiac hypertrophy in vivo. Cardiac-specific *Lin28a* knockout model ($Lin28a^{Cko}$) was generated by crossing $Lin28a^{fl/fl}$ mice with *Mlc2v-Cre* mice. Western blot analysis indicated that Cre-mediated conditional knockout of *Lin28a* reduced Lin28a protein level by at least 70% (Figure IIA in the online-only Data Supplement). The $Lin28a^{Cko}$ mice and control $Lin28a^{fl/fl}$ mice were then subjected to sham or TAC surgery. In the sham group, the gross morphology of $Lin28a^{Cko}$ hearts did not differ from that of $Lin28a^{fl/fl}$ hearts (Figure 2A).

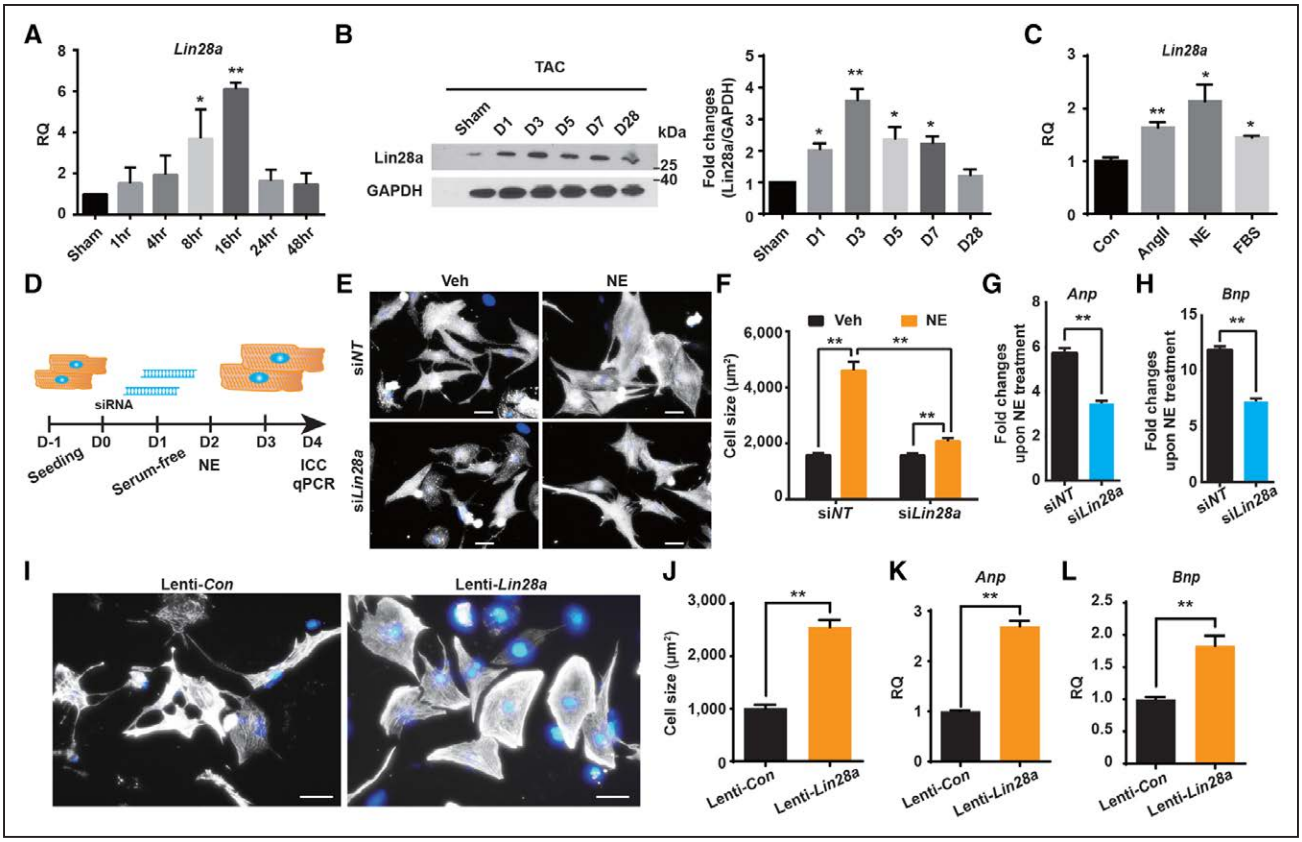

Figure 1. *Lin28a* plays a critical role in NE-induced cardiac hypertrophy.
A, The expression level of *Lin28a* mRNA in BL6 wild-type adult mice at indicated time points after TAC surgery. **B**, Western blot analysis and quantification of Lin28a protein expression in BL6 wild-type adult mice at indicated time points after TAC. **C**, The expression level of *Lin28a* mRNA in NRCMs 12 hours after angiotensin II (AngII), norepinephrine (NE), or fetal bovine serum (FBS) treatment. **D**, Schematic of siRNA-mediated *Lin28a* knockdown in NRCMs. **E**, Representative images of α-actinin–stained cardiomyocytes treated with NE, and transfected with negative control siRNA (si*NT*) or Silencer Select validated siRNA targeting *Lin28a* (si*Lin28a*) as indicated. Nuclei were counterstained with DAPI. Scale bar, 50 μm. **F**, Quantification of the cell surface area shown in **E**. **G** and **H**, Relative quantification (RQ) of fetal genes expression (*Anp, Bnp*) in cardiomyocytes treated with NE, and si*NT* or si*Lin28a* as indicated. **I**, Representative images of α-actinin–stained cardiomyocytes transduced with control lentiviruses (Lenti-*Con*) or lentiviruses expressing *Lin28a* (Lenti-*Lin28a*) as indicated. Nuclei are counterstained with DAPI. Scale bar, 50 μm. **J**, Quantification of the cell surface area shown in **I**. **K** and **L**, RQ of fetal genes expression (*Anp, Bnp*) in cardiomyocytes transduced with Lenti-*Con* or Lenti-*Lin28a* as indicated. Data are presented as mean±SEM. **P*<0.05; ***P*<0.01 by *t* test (**G** and **H** and **J** and **L**) or 1-way ANOVA (**A** through **C**) or 2-way ANOVA (**F**). Con indicates control; DAPI, 4′,6-diamidino-2-phenylindole; qPCR, quantitative polymerase chain reaction; NRCM, neonatal rat cardiomyocyte; si, small interfering; TAC, transverse aortic constriction; and Veh, vehicle.

In addition, we did not observe significant differences in the heart to body weight ratio between *Lin28a*^{Cko} mice and *Lin28a*$^{fl/fl}$ mice (5.40±0.06 versus 5.34±0.15 mg/g, *P*>0.05; Figure 2B). In contrast, TAC induced a significant increase in the size of *Lin28a*$^{fl/fl}$ hearts, and this TAC-induced hypertrophic growth was substantially suppressed by cardiac ablation of *Lin28a* (Figure 2A). *Lin28a*^{Cko} mice consistently demonstrated substantially decreased heart to body weight ratio in comparison with the *Lin28a*$^{fl/fl}$ mice after TAC surgery (7.84±0.29 versus 9.86±0.48 mg/g, *P*<0.05; Figure 2B). To further evaluate the effect of cardiac-specific *Lin28a* ablation on TAC-induced cardiac hypertrophy, we measured myocardial wall thickness of *Lin28a*^{Cko} and *Lin28a*$^{fl/fl}$ hearts at end-diastole (Figure 2C). At baseline, the thickness of *Lin28a*^{Cko} myocardial wall, including both left ventricular posterior wall and interventricular septum, was comparable to that of their control *Lin28a*$^{fl/fl}$ littermates (left ventricular posterior wall thickness: 0.79±0.03 versus 0.78±0.02 mm, *P*>0.05; interventricular septum thickness: 0.78±0.03 versus 0.76±0.02 mm, *P*>0.05; Figure 2D and 2E). Although both dimensions were substantially increased in *Lin28a*$^{fl/fl}$ hearts by TAC at 1 week postsurgery, *Lin28a*^{Cko} hearts exhibited only a mild increase in left ventricular wall thickness in response to TAC. Two and 4 weeks after TAC, the difference in the myocardial wall thickness between the 2 genotypes was even greater. For instance, at 4 weeks after TAC, left ventricular posterior wall thickness and interventricular septum thickness increased by 90.2% and 91.5%, respectively, in *Lin28a*$^{fl/fl}$ mice relative to baseline, whereas these dimensions increased only by 28.5% and 30.1%, respectively, in *Lin28a*^{Cko} mice (Figure 2D and 2E).

At the cellular level, pathological cardiac hypertrophy is characterized by an increase in cardiomyocyte size. To determine if the attenuation of hypertrophy by the loss of *Lin28a* function was attributable to the alteration in cardiomyocyte size, we labeled cardiomyocytes

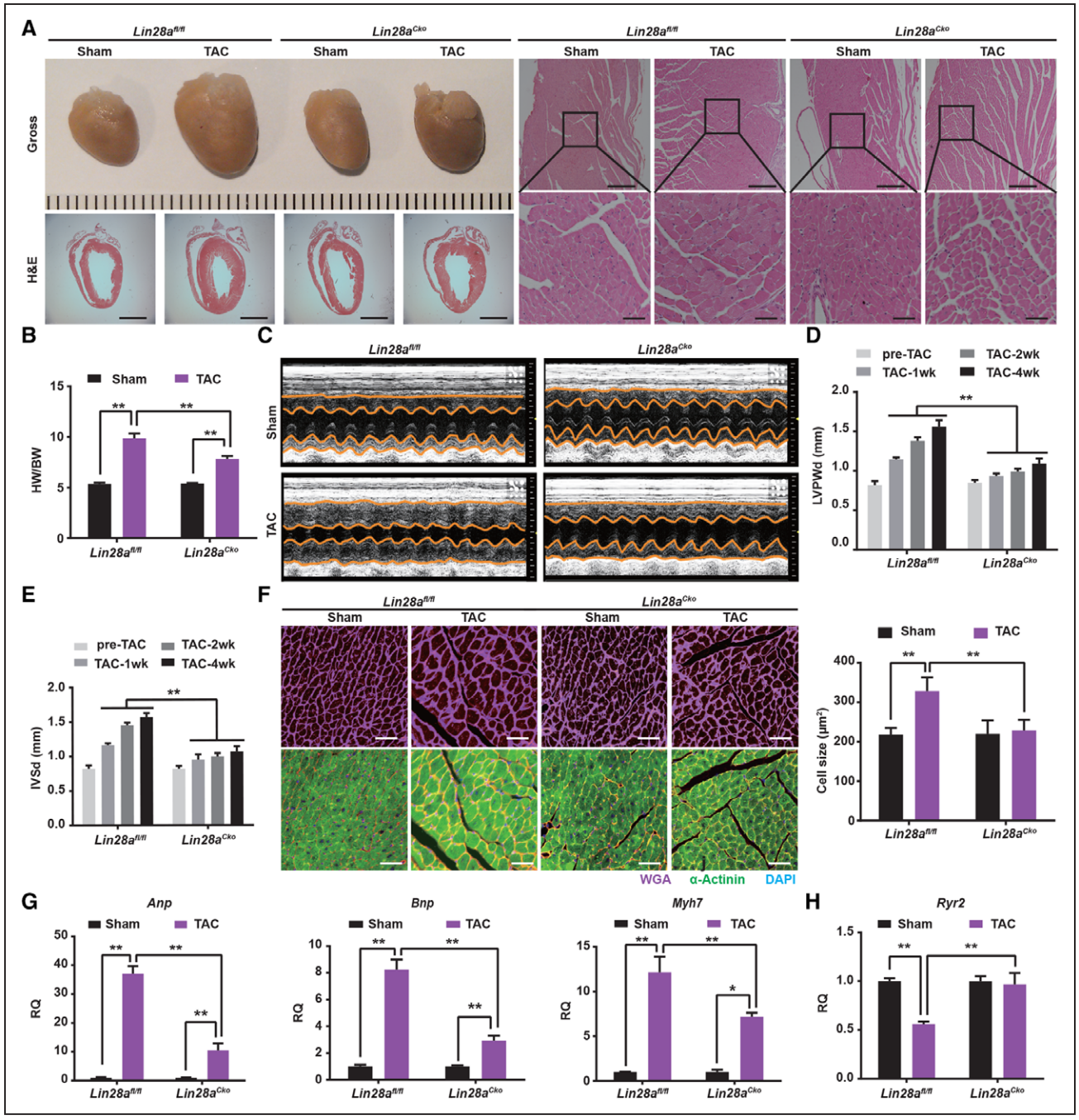

Figure 2. Cardiac conditional knockout of *Lin28a* attenuates pressure overload–induced cardiac hypertrophy.
A, Representative images of gross heart morphology and H&E-stained longitudinal sections of *Lin28a*^{Cko} or *Lin28a*$^{fl/fl}$ hearts at 4 weeks after TAC or sham operation. Scale bar in H&E gross image, 3 mm. Scale bar in H&E section, 500 μm. Scale bar in zoomed-in images, 100 μm. **B**, Heart weight to body weight (HW/BW) ratio at 4 weeks after TAC or sham operations. **C**, Representative examples of M-mode echocardiography of *Lin28a*^{Cko} and *Lin28a*$^{fl/fl}$ hearts under pressure overload. **D** and **E**, Quantification of end-diastolic posterior wall thickness (LVPWd; **D**) or end-diastolic interventricular septal wall thickness (IVSd; **E**) of *Lin28a*^{Cko} and *Lin28a*$^{fl/fl}$ hearts at 1 week, 2 weeks, and 4 weeks after sham or TAC operations. **F**, Representative images of heart sections from *Lin28a*^{Cko} mice or their *Lin28a*$^{fl/fl}$ littermates at 4 weeks after sham or TAC operations. The heart sections were immunostained with wheat germ agglutinin (WGA) in purple, α-actinin in green, and DAPI in blue. Scale bar, 100 μm. Quantification of the cross-sectional area of the cardiomyocytes shown in bar graph. **G**, RQ of the fetal gene expression (*Anp, Bnp, Myh7*) in *Lin28a*^{Cko} and *Lin28a*$^{fl/fl}$ hearts at 7 days after sham or TAC operations. **H**, RQ of calcium-handling gene ryanodine receptor type 2 (*Ryr2*) expression in *Lin28a*^{Cko} and *Lin28a*$^{fl/fl}$ hearts at 7 days after sham or TAC operations. Data are presented as mean±SEM. *P<0.05, **P<0.01 by 2-way ANOVA (**B** and **D** through **H**). DAPI indicates 4′,6-diamidino-2-phenylindole; H&E, hematoxylin and eosin; RQ, relative quantification; and TAC, transverse aortic constriction.

with wheat germ agglutinin and α-actinin double-immunostaining (Figure 2F). No significant difference was found in cardiomyocyte size between sham-operated *Lin28a*^{Cko} and *Lin28a*$^{fl/fl}$ hearts (220.30±8.75 versus 218.57±4.62, P>0.05; Figure 2F). However, cardiac ablation of *Lin28a* significantly suppressed TAC-induced enlargement of myocyte size (229.32±6.84 versus 328.14±8.92, P<0.01; Figure 2F).

We examined the effect of *Lin28a* ablation on cardiac hypertrophic marker genes expression. The upregulation of the fetal genes, including *Anp*, *Bnp*, and *Myh7*, observed in the hypertrophic hearts of *Lin28a*$^{fl/fl}$ mice was significantly suppressed in TAC-operated *Lin28a*^{Cko} hearts (Figure 2G). We also determined the expression of genes involved in cardiac function. The expression levels of ryanodine receptor 2 (*Ryr2*) and ATPase sarcoplasmic/endoplasmic reticulum Ca^{2+} transporting 2 (*Serca2*) were well preserved in TAC-operated *Lin28a*^{Cko} but not in *Lin28a*$^{fl/fl}$ hearts subjected to TAC (Figure 2H and Figure IIB in the online-only Data Supplement). Similar alterations in the expression seem to hold true also for several other genes important for cardiac contractility or function, such as phospholamban (*Pln*), ATP synthase, and myosin light chain (*Myl*; Figure IIC in the online-only Data Supplement), suggesting a potential beneficial effect of cardiac *Lin28a* ablation under pressure overload. Together, our studies demonstrate that *Lin28a* plays a critical role in both pressure overload and agonist-induced cardiac hypertrophy.

Loss of Cardiac *Lin28a* Attenuated Pressure Overload–Induced Cardiac Remodeling

Cardiac fibrosis is a maladaptive response to pressure overload and contributes to the transition from hypertrophy toward intractable heart failure.[20,21] We performed Picrosirius red staining to assess interstitial and perivascular fibrosis at 4 weeks after TAC. Under basal condition, neither *Lin28a*$^{fl/fl}$ nor *Lin28a*^{Cko} mice showed any sign of cardiac fibrosis (0.68±0.14% versus 0.75±0.15%, P>0.05; Figure 3A). It is notable that TAC significantly increased fibrosis in interstitial and perivascular areas in *Lin28a*$^{fl/fl}$ hearts but not in *Lin28a*^{Cko} hearts (Figure 3A). This observation was further confirmed by analysis of collagen content with polarized light, which revealed collagen type I in yellow (Figure 3B).

Transforming growth factor β signaling constitutes one of the most important signaling pathways required for cardiac fibrosis.[22,23] Transforming growth factor β signaling induces activation of cardiac fibroblast and subsequent fibrogenesis, in part, through its downstream mediator connective tissue growth factor (*Ctgf*).[24,25] It is interesting to note that gene expression analysis revealed that TAC-induced upregulation of transforming growth factor β signaling components and *Ctgf* was suppressed by loss of *Lin28a* (Figure IID in the online-only Data Supplement), suggesting that reduced activation of transforming growth factor β signaling may underlie the decreased fibrosis in the *Lin28a*^{Cko} hearts after TAC. We then examined the expression of genes more directly involved in fibrosis. Collagen type I α1 (*Col1a1*) and collagen type III α1 (*Col3a1*) encode the major collagen types in cardiac fibrotic tissue. Consistent with Picrosirius red staining, we observed a significant upregulation of both *Col1a1* and *Col3a1* at 4 weeks after TAC, and this upregulation was attenuated in *Lin28a*^{Cko} hearts (Figure 3C and 3D, Figure IID in the online-only Data Supplement, and Table I in the online-only Data Supplement). Collagen turnover and homeostasis in the heart is also affected by the levels of matrix metalloproteinases and tissue inhibitors of metalloproteinase. Although the expression levels of matrix metallopeptidase 2 (*Mmp2*) and matrix metallopeptidase 9 (*Mmp9*) remained comparable between TAC-operated *Lin28a*^{Cko} and *Lin28a*$^{fl/fl}$ hearts (Figure 3E and 3F), the expression of tissue inhibitor of metalloproteinase 1 (*Timp1*) and *Timp2* was significantly higher in *Lin28a*$^{fl/fl}$ control hearts than in *Lin28a*^{Cko} hearts after TAC (Figure 3G, Figure IID in the online-only Data Supplement, and Table I in the online-only Data Supplement). Our findings thus suggest that a decrease in the synthesis and an increase in the degradation of collagen may contribute to the reduction in fibrosis observed in *Lin28a*^{Cko} hearts subjected to TAC.

Cardiac hypertrophy is a major risk factor for the development of heart failure, eventually leading to ventricular dilation and dysfunction.[1,3] We performed echocardiographic measurement to assess long-term cardiac structural remodeling and function. At baseline, both *Lin28a*^{Cko} and *Lin28a*$^{fl/fl}$ mice showed comparable left ventricle diastolic dimension (3.36±0.09 versus 3.27±0.18 mm, P>0.05; Figure 3H) and normal cardiac function (ejection fraction, 83.01±1.54 versus 79.10±2.48, P>0.05; Figure 3I). In line with blunted hypertrophic growth, structural remodeling as indicated by LVID was alleviated in *Lin28a*^{Cko} hearts in comparison with *Lin28a*$^{fl/fl}$ hearts after TAC (Figure 3J through 3L). Concomitantly, the TAC-operated *Lin28a*^{Cko} hearts exhibited reduced left ventricular end-diastolic volume (Figure 3M) and end-systolic volume (Figure 3N). It is more important that *Lin28a*^{Cko} mice displayed preservation of ventricular systolic function as evidenced by their significantly reduced decline in ejection fraction and fraction shortening (Figure 3O and 3P). The survival rate of the *Lin28a*^{Cko} mice was improved consistently (Figure 3Q). The improvement of cardiac performance may result from a combination of increased contractility and decreased fibrotic remodeling (Figure 3A through 3D and Figure IIC and IID in the online-only Data Supplement). Together, loss of *Lin28a* ameliorates pressure overload–induced cardiac dysfunction and improved long-term survival.

Cardiac Ablation of *Lin28a* Mitigated Pressure Overload–Induced Alterations in Cardiac Transcriptomes

Given the well-known function of Lin28a in blocking *let-7* biogenesis,[26,27] we determined if *let-7* miRNAs participated in Lin28a-mediated cardiac hypertrophy. Consistent with a previous report,[28] several members of the *let-7* family were found to be upregulated in control

 Circulation. 2019;139:1725–1740. DOI: 10.1161/CIRCULATIONAHA.118.037803

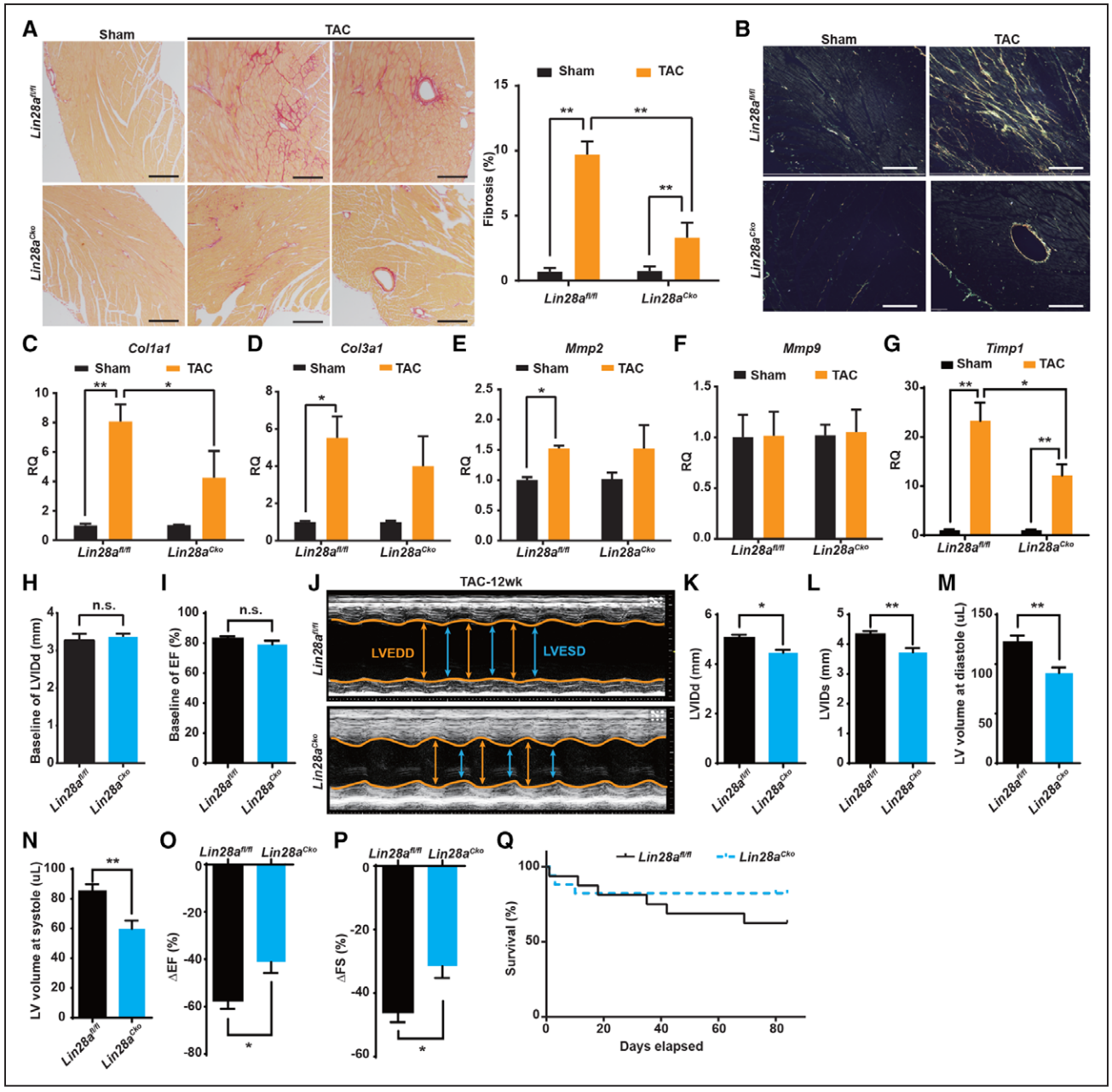

Figure 3. Pressure overload–induced cardiac fibrosis and cardiac dysfunction are alleviated by cardiac-specific knockout of *Lin28a*.
A, Representative images of Picrosirius red–stained sections from *Lin28a*^{Cko} or *Lin28a*$^{fl/fl}$ hearts at 4 weeks after sham or TAC operations. Scale bar, 500 μm. Quantification of cardiac fibrotic tissues in red is shown to the right. **B**, Representative images of Picrosirius red–stained sections from *Lin28a*^{Cko} or *Lin28a*$^{fl/fl}$ hearts at 4 weeks after sham or TAC operations visualized under polarized light microscopy. Collagen type I is shown in yellow-orange. Collagen type III is shown in green. Scale bar, 500 μm. **C** through **G**, RQ of collagen type I α1 (*Col1a1*; **C**), collagen type III α1 (*Col3a1*; **D**), matrix metallopeptidase 2 (*Mmp2*; **E**), matrix metallopeptidase 9 (*Mmp9*; **F**), and tissue inhibitor of metalloproteinase 1 (*Timp1*; **G**) expression in *Lin28a*^{Cko} and *Lin28a*$^{fl/fl}$ hearts at 7 days after sham or TAC operations. **H** and **I**, Quantification of left ventricle diastolic diameter (LVIDd; **H**) and ejection fraction (EF; **I**) of *Lin28a*^{Cko} and *Lin28a*$^{fl/fl}$ hearts at baseline. **J**, Representative examples of M-mode echocardiography of *Lin28a*^{Cko} and *Lin28a*$^{fl/fl}$ hearts under pressure overload at 12 weeks after TAC surgery. **K** through **P**, Changes in LVIDd (**K**), left ventricle systolic diameter (LVIDs; **L**), left ventricular volume at diastole (**M**) and systole (**N**), EF (**O**), and fraction shortening (FS; **P**) in *Lin28a*^{Cko} mice and their *Lin28a*$^{fl/fl}$ littermates at 12 weeks after TAC surgery. **Q**, Survival rates of *Lin28a*^{Cko} mice and their *Lin28a*$^{fl/fl}$ littermates after sham or TAC operations. Data are presented as mean±SEM. **P*<0.05, ***P*<0.01; n.s., not significant by *t* test (**H** and **I** and **K** through **P**), or 2-way ANOVA (**A** and **C** through **G**). LV indicates left ventricular; RQ, relative quantification; and TAC, transverse aortic constriction.

hearts subjected to TAC surgery (Figure IIIA through IIIC in the online-only Data Supplement). However, cardiac-specific ablation of *Lin28a* did not further increase the expression of these *let-7* miRNAs. In addition, comparison of *Lin28a* and *let-7* expression revealed that they were both upregulated after TAC during a similar time window (Figure IIIA through IIIC in the online-only Data Supplement; see also Figure 1A and 1B), suggesting that the effect of Lin28a on cardiac hypertrophy is unlikely to be mediated by *let-7*. In addition to the established role in inhibiting *let-7* biogenesis, Lin28a also directly binds to mRNAs to enhance mRNA stabil-

ity or translation efficiency.[17,29–31] To identify potential *let-7*–independent mechanisms underlying *Lin28a*-mediated cardiac hypertrophy, we conducted whole genome-wide RNA deep sequencing to profile the transcriptomes of *Lin28a*^{Cko} and control hearts at 5 days after sham or TAC, a time point shortly after Lin28a exhibited a peak level of upregulation in response to TAC (Figure 1B). Boxplot, MA plots, and clustering of the RNA-sequencing data confirmed the consistency between the biological repeats for each condition (Figure IVA through IVD in the online-only Data Supplement). Although the cardiac transcriptomes of *Lin28a*^{Cko} and *Lin28a*$^{fl/fl}$ mice were similar (Figure IVE in the online-only Data Supplement) and clustered closely together under baseline (Figure IVC and IVD in the online-only Data Supplement), unsupervised hierarchical clustering analysis indicated that TAC markedly altered cardiac transcriptome of *Lin28a*$^{fl/fl}$ mice (Figure IVC and IVD in the online-only Data Supplement and Figure VA in the online-only Data Supplement). The cardiac transcriptome of TAC-operated *Lin28a*^{Cko} mice, however, more closely resembled that of sham-operated controls than that of TAC-operated *Lin28a*$^{fl/fl}$ mice, suggesting that the effect of mechanical stress on cardiac transcriptome was mitigated by loss of *Lin28a* function (Figure IVC and IVD in the online-only Data Supplement and Figure VA in the online-only Data Supplement).

We identified a total of 4706 genes differentially expressed between TAC-operated *Lin28a*^{Cko} and *Lin28a*$^{fl/fl}$ cardiac samples (Figure VB in the online-only Data Supplement). Functional annotation of these differentially expressed genes using DAVID tools (Database for Annotation, Visualization and Integrated Discovery) revealed that several previously reported pathways, such as metabolic, phosphoinositide-3-kinase–Akt and mitogen-activated protein kinase signaling pathways were affected by loss of *Lin28a* function (Figure 4A). It is notable that a close exploration of the differentially expressed metabolic gene sets using DAVID, pathway analysis (Ingenuity pathway analysis), and gene set enrichment analysis demonstrated extensive alterations in multiple metabolic processes, including fatty acid oxidation, tricarboxylic acid (TCA) cycle, oxidative phosphorylation, glycolysis, and pentose phosphate pathways (Figure 4B through 4E, Figure VC and VD in the online-only Data Supplement, and Figure VI in the online-only Data Supplement), suggesting that loss of *Lin28a* function had a profound effect on cardiac metabolism during hypertrophy. In particular, both gene set enrichment and Ingenuity pathway analyses indicated that TAC-induced downregulation of oxidative phosphorylation was alleviated by cardiac ablation of *Lin28a* (Figure 4C through 4E and Figure VI in the online-only Data Supplement). For instance, detailed gene expression analysis demonstrated that TAC-operated *Lin28a*^{Cko} hearts showed significant higher expression of the genes encoding mitochondrial oxidation complex, such as succinate dehydrogenase (*Sdh*), NADH:ubiquinone oxidoreductase (*Nduf*), cytochrome c oxidase (*Cox*) and ubiquinol-cytochrome c reductase (*Uqcr*) in comparison with *Lin28a*$^{fl/fl}$ hearts subjected to TAC (Figure IIE in the online-only Data Supplement), which may contribute to the improvement of cardiac function observed in *Lin28a*^{Cko} hearts subjected to TAC. Quantitative reverse transcription polymerase chain reaction analysis consistently revealed a similar trend of metabolic gene expression changes between control NRCMs, NRCMs treated with NE, and NRCMs treated with NE and si*Lina28a* (Figure 4F).

Identification of Pck2 as a Direct Target of Lin28a

To gain insight into how Lin28a regulates pathological hypertrophic growth, we sought to identify direct targets of Lin28a among the differentially expressed genes that responded to loss of *Lin28a* function after TAC. It is interesting to note that several genome-wide studies have attempted to identify direct targets of Lin28a. We reanalyzed the cross linking and immunoprecipitation–sequencing data generated by Cho et al,[32] and found that 1249 genes were significantly enriched in Lin28a pull-down components. These 1249 genes were potentially direct targets of Lin28a because their mRNAs were directly bound to Lin28a protein. Among the differentially expressed genes in our RNA-sequencing data (total 4706 genes), and potential Lin28a direct targets (total 1249 genes), 47 and 19 of which were involved in the most enriched metabolic and phosphoinositide-3-kinase–AKT pathways (Figure 5A). We focused on the overlapping candidate genes (Figure 5A) and performed quantitative reverse transcription polymerase chain reaction to further assess their expression in response to pathological hypertrophic stimuli. Fifteen of these candidate genes showed a similar response to mechanical overload in vivo and neurohumoral stimuli in vitro (Figure 5B). We performed RNA immunoprecipitation assay to test whether these candidates were directly bound by Lin28a in cardiomyocytes. FLAG-tagged Lin28a was overexpressed in cardiomyocytes and was pulled down by anti-FLAG antibody (Figure 5C). Quantitative polymerase chain reaction analysis was then performed to determine the level of transcripts in the protein-RNA complex pulled down by anti-FLAG antibody in comparison with that by anti-IgG controls (Figure 5D). *Pck2* was the most enriched candidate transcripts in the anti-FLAG fraction (Figure 5D, Figure VIIA in the online-only Data Supplement and Tables I and II in the online-only Data Supplement). To further examine the physical interaction between Lin28a and *Pck2* mRNA, lentiviruses expressing FLAG-tagged *Lin28a* were transduced into adult mouse hearts via myocardial injection. RNA immu-

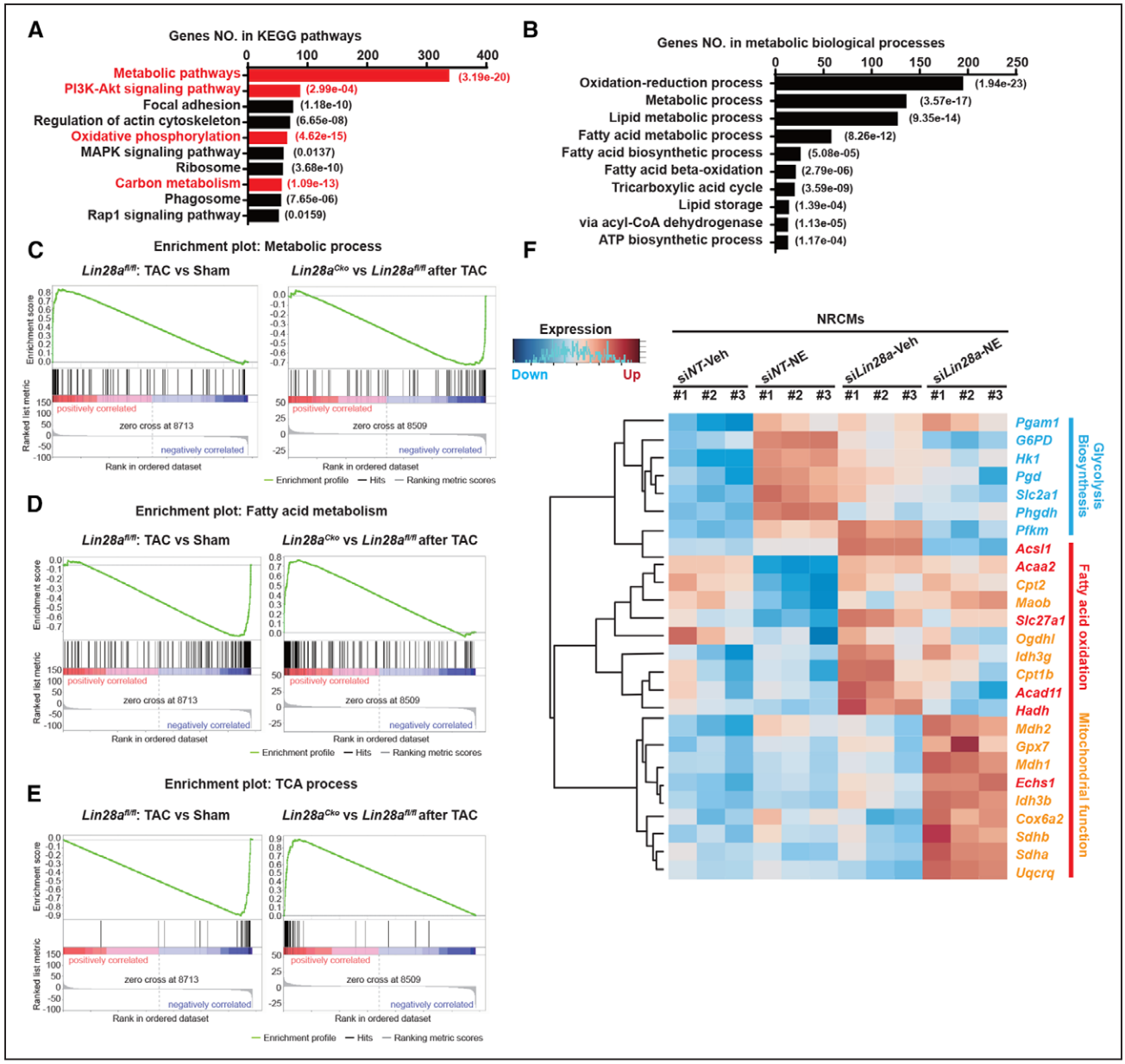

Figure 4. Loss of *Lin28a* mitigated the effect of TAC on cardiac transcriptome.
A, Functional enrichment analysis using DAVID tools. Gene Ontology (GO) annotation of the differentially expressed genes from the hypertrophied *Lin28a*^{Cko} and *Lin28a*$^{fl/fl}$ hearts. Metabolism-related terms are labeled in red. **B**, GO analysis of the metabolic processes affected in the hypertrophied *Lin28a*^{Cko} and *Lin28a*$^{fl/fl}$ hearts. **C** through **E**, Gene set enrichment analysis (GSEA) showing the gene sets of metabolic process (**C**), fatty acid metabolism (**D**), and TCA process (**E**) affected by cardiac deletion of *Lin28a* in cardiac hypertrophy. **F**, Heatmaps of the relative expression of the differentially expressed genes identified in RNA-sequencing in cardiomyocyte transfected with negative control siRNA (si*NT*) or *Lin28a* siRNA (si*Lin28a*) under NE treatment for 48 hours in vitro. CoA indicates coenzyme A; DAVID, Database for Annotation, Visualization and Integrated Discovery; KEGG, Kyoto Encyclopedia of Genes and Genomes; NE, norepinephrine; MAPK, mitogen-activated protein kinase; NRCM, neonatal rat cardiomyocyte; PI3K, phosphoinositide-3-kinase; TAC, transverse aortic constriction; TCA, tricarboxylic acid; and Veh, vehicle.

noprecipitation demonstrated that *Pck2* mRNA was enriched in the anti-FLAG pull-down fraction (Figure VIIB in the online-only Data Supplement). Through these selection criteria, we were able to narrow down to *Pck2* as the most prominent downstream target of Lin28a in cardiomyocytes (Figure 5D). To validate this finding, we performed quantitative polymerase chain reaction analysis with RNA samples from the TAC-operated *Lin28a*$^{fl/fl}$ hearts, and found that these hearts exhibited a significantly upregulated *Pck2* level in comparison with sham-operated *Lin28a*$^{fl/fl}$ hearts (Figure 5E). Cardiac-specific knockout of *Lin28a* mitigated this TAC-induced upregulation of *Pck2* (Figure 5E). Likewise, *Pck2* expression was markedly upregulated in NE-treated hypertrophic NRCMs (Figure 5F). Furthermore, overexpression of *Lin28a* in NRCMs resulted in a remarkable increase in *Pck2* expression at both transcript and protein levels, whereas silencing of *Lin28a* downregulated *Pck2* expression by 46% in NRCMs (Figure 5G and 5H and Figure VIIC in the online-only Data Supplement). These

ORIGINAL RESEARCH ARTICLE

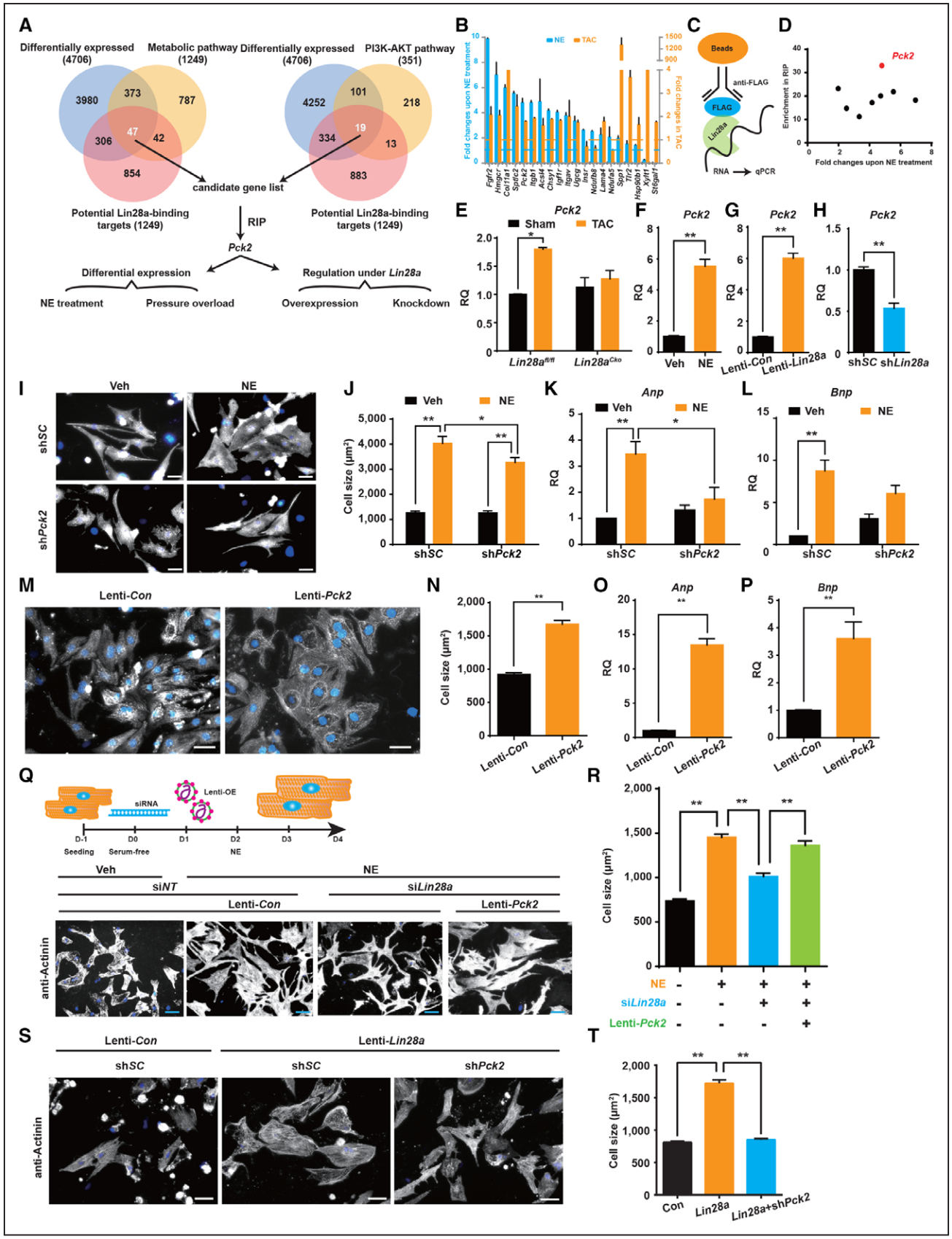

Figure 5. Pck2 functions as a direct downstream mediator of Lin28a in cardiomyocyte hypertrophic growth.
A, Workflow to identify and further validate the direct targets of Lin28a involved in metabolic regulation through analysis of our RNA-sequencing data and published CLIP-sequencing data. **B**, RQ of the upregulation of the top 20 candidate target genes in cardiomyocytes in response to pressure overload in vivo (in orange) or NE stimulation in vitro (in blue). (*Continued*)

data collectively demonstrate that *Pck2* mRNA is physically bound by Lin28a and its level is controlled by Lin28a during cardiac hypertrophy.

Genetic Interaction of *Lin28a* and *Pck2* in NE-Induced Cardiac Hypertrophy

We sought to determine whether a Lin28a/Pck2 axis existed in regulating cardiac hypertrophic growth. First, we examined the response of Pck2 to TAC surgery and found that Pck2 exhibited transient upregulation similar to that of Lin28a with its peak level of expression occurring at 5 to 7 days after TAC (Figure VIID and VIIE in the online-only Data Supplement; see also Figure 1A and 1B). Then, we addressed the requirement for *Pck2* in NE-induced NRCM hypertrophy. Analysis of NRCM size demonstrated that knocking down *Pck2* resulted in the attenuation of NE-induced increase in NRCM size and upregulation of *Anp*, *Bnp*, *Acta1*, and *Myh7* (Figure 5I through 5L, and Figure VIIF through VIIH in the online-only Data Supplement), indicating that Pck2 is required for the development of NE-induced cardiac hypertrophy. Conversely, overexpression of *Pck2* by transducing NRCMs with lentiviruses expressing *Pck2* (Lenti-*Pck2*) resulted in a similar, albeit less pronounced, NRCM hypertrophic growth phenotype to that of overexpressing *Lin28a* (Figure 5M through 5P and Figure VIII through VIIK in the online-only Data Supplement), and reactivated fetal gene expression indicated by the upregulation of *Anp*, *Bnp*, *Myh7*, and *Acta1* (Figure 5O and 5P and Figure VIIJ and VIIK in the online-only Data Supplement). Likewise, lentiviral-mediated *Pck2* overexpression in adult mouse hearts also led to enlargement of cardiomyocyte size and reactivation of fetal gene expression (Figure VIIIA through VIIIF in the online-only Data Supplement). Because knockdown of *Lin*28a and overexpression of *Pck2* resulted in opposite phenotypes, we asked if overexpressing *Pck2* could reverse the attenuation of NE-induced NRCM hypertrophy by the loss of *Lin28a* function. To this end, we introduced the NE-treated NRCMs with *siLin28a*, and subsequently transduced these cells with Lenti-*Pck2*. It is remarkable that we found that *Pck2* overexpression was sufficient to induce hypertrophic growth of the NE-treated NRCMs even in the absence of *Lin28a* function (Figure 5Q and 5R), suggesting that Pck2 acted epistatically to Lin28a to regulate NRCM hypertrophy. To directly determine the epistatic relationship of Lin28a and Pck2, we knocked down *Pck2* in Lenti-*Lin28a*–transduced NRCMs, and found that knockdown of *Pck2* suppressed Lin28a-induced NRCM hypertrophy (Figure 5S and 5T). The above data thus indicate that *Pck2* functions to mediate, at least in part, the effect of Lin28a in cardiac hypertrophic growth.

Lin28a/Pck2 Promotes Cardiac Glycolysis and Anabolic Synthesis

Because the hypertrophic heart features an increased reliance on glucose metabolism, we monitored the glycolytic capacity of NRCMs by measuring the extracellular acidification rate of the surrounding media (Figure 6A). As expected, NE treatment resulted in a significant increase in the glycolytic capacity of NRCMs in comparison with vehicle treatment (Figure 6B). Significantly enhanced NRCM glycolytic capacity was also observed in *Lin28a*- or *Pck2*-overexpressing NRCMs in comparison with the control cells (Figure 6B). This enhanced glycolytic metabolism was accompanied by compromised capacity to use palmitate as energy source (Figure IXA through IXD in the online-only Data Supplement), consistent with the data that cardiac deletion of *Lin28a* may improve the oxidative metabolism after TAC operation (Figure 4B through 4E and Figure VI in the online-only Data Supplement). Giving the ability of Lin28 and Pck2 to promote glycolysis, we examined the expression of glucose transporter and genes encoding key glycolytic enzymes and found significant upregulation of glucose transporter 1(*Slc2a1*), hexokinase 1(*Hk1*), and muscle pyruvate kinase (*Pkm*) on *Lin28* or *Pck2* overexpression (Figure IXE through IXH in the online-only Data Supplement). It is interesting to note that

Figure 5 Continued. **C**, Schematic overview of RNA immunoprecipitation against FLAG-tagged Lin28a in cardiomyocytes to determine enrichment of potential Lin28a binding targets. **D**, RQ of Lin28a target genes enrichment in the Lin28a protein-RNA complex determined by RNA immunoprecipitation (RIP) assay (*y* axis) and of Lin28a binding target genes upregulation in response to NE stimulation in cardiomyocytes (*x* axis). The dots represent the Lin28a target genes tested in **B**: *Acsl4, Chsy1, Hmgcr, Lama4, Pck2, Spp1, Sptlc2, St6gal1, Ugcg,* and *Xylt1*. **E**, RQ of *Pck2* expression in sham or TAC-operated *Lin28a*^{Cko} and *Lin28a*$^{fl/fl}$ hearts. **F**, RQ of *Pck2* expression level in vehicle or NE-treated cardiomyocytes. **G**, RQ of the upregulation of *Pck2* in *Lin28a*-overexpressing cardiomyocytes. **H**, RQ of *Pck2* expression in sh*SC*- or sh*Lin28a*-treated cardiomyocytes. **I**, Representative images of α-actinin–stained cardiomyocytes treated with NE, and sh*SC* or sh*Pck2* as indicated. Nuclei are counterstained with DAPI. Scale bar, 50 μm. **J**, Quantification of the surface area of the cells as shown in **I**. **K** and **L**, RQ of fetal genes expression (*Anp, Bnp*) in cardiomyocytes treated with NE, and transduced with sh*SC* or sh*Pck2* as indicated. **M**, Representative images of α-actinin–stained cardiomyocytes transduced with Lenti-*Con* or Lenti-*Pck2*. Nuclei are stained with DAPI. Scale bar, 50 μm. **N**, Quantification of the surface area of the cells as shown in **M**. For cell surface area quantification, >100 cells indiscriminately selected were measured in each group. **O** and **P**, RQ of fetal genes expression (*Anp, Bnp*) in cardiomyocytes transduced with Lenti-*Con* or Lenti-*Pck2*. **Q**, Schematic of lentivirus-mediated *Pck2* overexpression in the *Lin28a* knockdown cardiomyocytes under NE stimulation and representative images of α-actinin–stained cardiomyocytes treated by combinations of vehicle or NE, si*NT* or si*Lin28a*, and Lenti-Con or Lenti-*Pck2* as indicated. Nuclei were counterstained with DAPI. Scale bar, 50 μm. **R**, Quantification of the surface area of the cells as shown in **Q**. **S**, Representative images of α-actinin–stained cardiomyocytes transduced with combinations of Lenti-*Con* or Lenti-*Lin28a*, sh*SC* or sh*Pck2* as indicated. Nuclei were counterstained with DAPI. Scale bar, 50 μm. **T**, Quantification of the surface area of the cells as shown in **S**. Data are presented as mean±SEM. **P*<0.05, ***P*<0.01 by *t* test (**F** through **H**, and **N** through **P**), or 1-way ANOVA (**R** and **T**), or 2-way ANOVA (**E** and **J** through **L**). CLIP indicates cross linking and immunoprecipitation; DAPI, 4′,6-diamidino-2-phenylindole; NE, norepinephrine; PI3K, phosphoinositide-3-kinase; RQ, relative quantification; sh, short hairpin; si, small interfering; TAC, transverse aortic constriction; and Veh, vehicle.

ORIGINAL RESEARCH ARTICLE

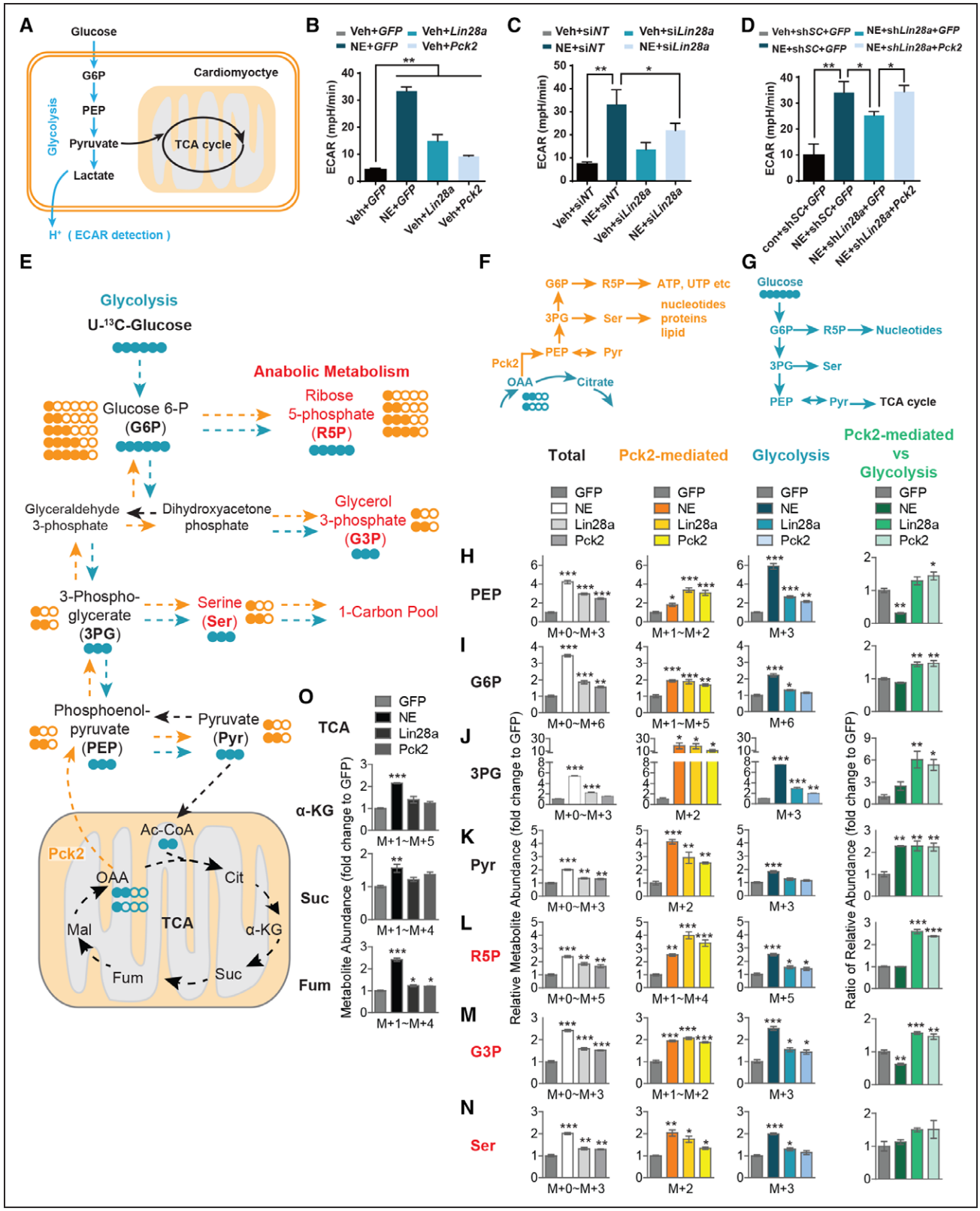

Figure 6. Lin28a/Pck2 promotes cardiac glycolysis and anabolic synthesis.
A, Schematic of extracellular acidification rate (ECAR) measurements in cardiomyocytes. **B**, Glycolytic capacity of cardiomyocytes with control (GFP) or lentivirus-mediated *Lin28a* overexpression (*Lin28a*) or *Pck2* overexpression (*Pck2*) under vehicle or NE treatment as indicated. **C**, Glycolytic capacity of cardiomyocytes treated with NE, and si*NT* or si*Lin28a* as indicated. **D**, Glycolytic capacity of cardiomyocytes treated with combinations of vehicle or NE, sh*SC* or sh*Lin28a* and GFP control or lentivirus-mediated *Pck2* overexpression (*Pck2*) as indicated. **E**, Schematic of metabolism of uniformly ^{13}C-labeled glucose. Glycolytic and Pck2-mediated metabolic fluxes are highlighted in blue and orange, respectively. **F**, Schematic of Pck2-mediated biosynthesis. **G**, Schematic of biosynthesis from glycolysis. (*Continued*)

knockdown of *Lin28a* suppressed NE-induced enhancement of cardiac glycolysis (Figure 6C).Gene expression analysis also consistently showed that the upregulation of the key glycolytic genes induced by NE was attenuated by knockdown of *Lin28a* or *Pck2* (Figure IXI through IXL in the online-only Data Supplement). We also evaluated the effect of *Pck2* overexpression on glycolytic rate of the NE- and si*Lin28a*-treated NRCMs. Extracellular acidification rate measurements demonstrated that *Pck2* overexpression could partly reverse the suppression of NE-induced enhancement of NRCM glycolysis by *Lin28a* knockdown (Figure 6D).

Next, we used stable isotope tracing of glucose to further determine the effects of *Lin28a* or *Pck2* overexpression on cardiac glycolysis. The incorporation of U-^{13}C-glucose was monitored by using liquid chromatography coupled to high-resolution mass spectrometry.[33] Metabolism of U-^{13}C-glucose is depicted in Figure 6E. Glycolytic and Pck2-mediated metabolic fluxes are highlighted in blue and orange, respectively (Figure 6E through 6G and Table III in the online-only Data Supplement). Consistent with the role of Pck2 in catalyzing the conversion of oxaloacetate (OAA) from TCA cycle to phosphoenolpyruvate, NE treatment, and *Lin28a* or *Pck2* overexpression resulted in a significant increase in the production of ^{13}C-labeled OAA-derived phosphoenolpyruvate (Figure 6F and 6H). Likewise, *Lin28a* or *Pck2* overexpression significantly increased the relative abundance of glycolytic metabolites, including glucose 6-phosphate and 3-phosphoglycerate (Figure 6I and 6J). It is interesting to note that this increase in glycolytic metabolite abundance was attributable to enhanced production of both U-^{13}C-glucose–derived and ^{13}C-labeled OAA-derived glycolytic metabolites (Figure 6F through 6K).

Pck2-mediated synthesis of phosphoenolpyruvate could be channeled to biosynthesis required for cell growth[34,35]; we determined the effect of *Lin28a*/*Pck2* overexpression on the synthesis of anabolic metabolites. Liquid chromatography/high-resolution mass spectrometry analysis demonstrated that *Lin28a* or *Pck2* overexpression led to significantly increased relative abundance of Pck2-mediated synthesis of OAA-derived ribose 5-phosphate (Figure 6L). This enhanced production of ribose 5-phosphate, in turn, contributed to an increased nucleotide synthesis as indicated by the upregulated levels of nucleotides, such as ATP and UTP (Figure XA through XC in the online-only Data Supplement). Cardiomyocyte hypertrophic growth also requires synthesis of lipids for the generation of biological membranes.[36] The production of OAA-derived glycerol 3-phosphate, an important starting material for de novo synthesis of glycerophospholipids, was remarkably enhanced on *Lin28a* or *Pck2* overexpression (Figure 6M). Serine is the essential precursor for nucleotides, proteins, and lipids during cell growth.[37] We addressed whether overexpression of *Lin28a* or *Pck2* could promote the production of OAA-derived serine. Among all the ^{13}C-labeled serine, the m+2 fractions directly generated from OAA mediated by Pck2 increased by 1.75±0.14– and 1.34±0.05–fold (Figure 6N), respectively, in *Lin28a*- or *Pck2*-overexpressing cardiomyocytes. In addition to the increased production of OAA-derived anabolic metabolites, the levels of the fully labeled anabolic metabolites were also significantly elevated (Figure 6E and 6H through 6N). It is worth noting that the increase in glycolytic and anabolic metabolites in NE-treated, *Lin28a*- or *Pck2*-overexpressing cardiomyocytes was not at the expense of TCA cycle intermediates, because the levels of the major TCA metabolites such as α-ketoglutarate, succinate, and fumarate remained comparable to, if not higher than, those in the control cardiomyocytes (Figure 6O). Although the enhanced production of anabolic metabolites may be explained by the increased abundance of glycolytic intermediates, which serve as the precursors for biosynthesis, we found that *Lin28*/*Pck2* overexpression also upregulated the expression of genes encoding the key metabolic enzymes in the pentose phosphate pathway, serine biosynthesis, and one-carbon metabolic pathways, including glucose-6-phosphate dehydrogenase (*G6pd*), phosphogluconate dehydrogenase (*Pgd*), phosphoglycerate dehydrogenase (*Phgdh*), phosphoserine aminotransferase 1 (*Psat1*), methylenetetrahydrofolate dehydrogenase 1 like (*Mthfd1l*), and methylenetetrahydrofolate dehydrogenase 2 (*Mthfd2*; Figure XD through XI in the online-only Data Supplement). This increase in the expression of one-carbon metabolic genes *Mthfd1l* and *Mthfd2* suggests that the serine that enters one-carbon metabolism may be further used within the activated folate cycle to support cell growth.[38] Conversely, knockdown of *Lin28a* or *Pck2* and cardiac ablation of *Lin28a* attenuated the upregulation of these key biosynthetic genes induced by NE and TAC, respectively (Figure XJ through XP in the online-only Data Supplement). These observations are consistent with gene set enrichment and Ingenuity pathway analyses of the RNA-sequencing data, showing that the biosynthetic pathways are enriched in the

Figure 6 Continued. **H** through **O**, Relative abundance of glycolytic-derived (blue) or OAA-derived (orange) metabolic intermediates in NE-treated, *Lin28a*- or *Pck2*-overexpressing cardiomyocytes relative to GFP control, including PEP (**H**), G6P (**I**), 3PG (**J**), Pyr (K), R5P (**L**), G3P (**M**), Ser (**N**), and TCA intermediates α-KG, Suc, Fum (**O**) generated from U-^{13}C-Glucose or diverted from TCA cycle by Pck2. The sum of the indicated fractions from M+0 to M+n was labeled under the corresponding plots. Data are presented as mean±SEM. **P*<0.05, ***P*<0.01, ****P*<0.001 by 1-way ANOVA (**B** through **D** and **H** through **O**). Fum indicates fumaratep; G3P, glyceraldehyde 3-phosphate; G6P, glucose 6-phosphate; GFP, green fluorescent protein; α-KG, α-ketoglutarate; NE, norepinephrine; OAA, oxaloacetate; PEP, phosphoenolpyruvate; 3PG, 3-phosphoglycerate; Pyr, pyruvate; R5P, ribose 5-phosphate; Ser, serine; sh, short hairpin; si, small interfering; Suc, succinate; TCA, tricarboxylic acid; and Veh, vehicle.

differentially expressed genes between TAC-operated *Lin28a*^{Cko} and control hearts (Figures VI and XQ in the online-only Data Supplement). Our data thus implicate Lin28a/Pck2-dependent enhancement of biosynthesis and glycolysis as a mechanism for cardiomyocyte hypertrophic growth.

DISCUSSION

Hypertrophic response to pathological stimuli is a complex biological process that involves transcriptional, posttranscriptional, and epigenetic regulation of the cardiac genome. Despite substantial progress in our understanding of the molecular and physiological basis of this detrimental process, much remains to be learned. Here, we report that Lin28a plays a pivotal role in pathological cardiac hypertrophy. Cardiac-specific deletion of *Lin28a* blunted pressure overload–induced cardiac hypertrophy and suppressed cardiac fibrosis. It is more important that *Lin28a* conditional knockout mice showed preserved cardiac function and improved long-term survival. Likewise, in an in vitro model of cardiac hypertrophy, knockdown of *Lin28a* attenuated NE-induced hypertrophy, while overexpressing *Lin28a* alone was sufficient to stimulate cardiomyocyte hypertrophic growth. Further study indicated that the role of *Lin28a* in cardiac hypertrophic growth was mediated at least in part by *Pck2*, which in turn promoted cardiac glycolysis and biosynthesis during cardiac hypertrophy. Although knockdown of *Pck2* suppressed Lin28a-induced cardiomyocyte hypertrophic growth, overexpressing *Pck2* reversed the attenuation of NE-induced hypertrophy by loss of *Lin28a* function. Together, our study indicated that Lin28a acts as a crucial regulator of pathological cardiac hypertrophy via regulating cardiomyocyte glycolysis and biosynthesis.

Lin28 was initially characterized in *Caenorhabditis elegans* for its role in controlling developmental timing. The vertebrate genome contains 2 Lin28 paralogues, Lin28a and Lin28b. Over the past 3 decades, the Lin28 paralogues have been primarily implicated in promoting pluripotency and carcinogenesis,[12] yet its roles in terminally differentiated organs such as heart, especially under stress conditions, remain largely unknown. In this study, we found that the expression of *Lin28a,* but not *Lin28b,* was stimulated by pathological hypertrophic stimuli. This observation is reminiscent of the differential stabilization of Lin28a through mitogen-activated protein kinase–dependent posttranscriptional mechanism.[39] Although it is not clear whether Lin28a could also be stabilized at the protein level during pathological cardiac hypertrophy, our finding highlights a previously unappreciated differential regulation of *Lin28* paralogous at the transcriptional level. The *Lin28* paralogues are thought to have arisen by gene duplication, yet their distinct and overlapping functions still await to be fully characterized. In light of the recent reports that Lin28a is primarily localized in the cytoplasm while Lin28b is predominantly found in the nucleus,[40] it is conceivable the relative distinct subcellular localization might contribute to the distinct roles the 2 Lin28 proteins play in regulating diverse cellular processes.

During pathological hypertrophy, the early-response genes, such as *c-Fos, c-Jun,* and *c-Myc*, are generally induced within 30 minutes after pathological stimulation.[41] Our observation that the induction of *Lin28a* slightly lagged behind that of the early-response genes suggests that *Lin28a* could be directly activated by these factors. Indeed, previous studies indicated that c-Myc binds to the promoter of *Lin28a* and activates its transcription in cancer cells.[18,19] It will be interesting to determine if *Lin28a* is a direct target of c-Myc in cardiac tissue during pathological hypertrophy. Pathological hypertrophic stimuli induce extensive and dynamic changes in cardiac transcriptome at both transcriptional and posttranscriptional levels. miRNA-mediated RNA decay has been shown to be a critical component of the posttranscriptional mechanisms to fine-tune the cardiac transcriptome, yet several lines of evidence imply that increased mRNA stability may also contribute to the dynamic regulation of cardiac transcriptome during hypertrophic growth.[42,43] Lin28a directly binds to diverse mRNAs[31] and enhances their stability and translation efficiency.[17,44] This regulatory mechanism of gene expression could poise the cells to readily adapt to external challenges. Our data consistently showed that cardiac conditional knockout of *Lin28a* largely mitigated the alterations in cardiac transcriptome induced by pressure overload. Thus, Lin28a-mediated transcript stabilization represents another type of posttranscriptional regulatory mechanism during pathological hypertrophy.

Metabolic reprogramming is one of the major hallmarks of cardiac hypertrophy, because the hypertrophic heart relies more on glucose metabolism than fatty acid oxidation.[6] It is interesting to note that most of the genes affected by the loss of *Lin28a* at the early phase of cardiac hypertrophy are enriched in metabolism and related pathways. In addition, glycolytic capacity assay and metabolic flux analysis using ^{13}C-glucose further demonstrated that Lin28a functioned to increase glycolysis and anabolic pathways at the expense of compromised oxidative capacity in the hypertrophied cardiomyocytes. Our findings are thus not only consistent with previous findings that Lin28a functions as primal regulator of glucose metabolism in diabetes mellitus,[14] wound healing,[15] oncogenesis,[16] and pluripotency,[12] but also highlight its distinct role in the adult heart under stress conditions. It is more important that we identified *Pck2* as a critical direct target of Lin28a in cardiomyocytes. Manipulation of *Pck2* expression recapitulated the phenotypes of manipulating *Lin28a* knockdown or overexpression, demonstrating the crucial role

of Lin28a/Pck2 axis in metabolic reprogramming during cardiac hypertrophy. Cardiomyocytes subjected to hypertrophic stimuli exhibit increased demands for protein, lipid, and nucleotide synthesis to fulfill the requirement for cell growth.[6] Pck2 diverts carbon substrates from the TCA cycle to glycolysis flux, thereby enhancing anabolic synthesis from glycolytic intermediates to support cardiomyocyte growth. Recent studies have shown that phosphoenolpyruvate carboxykinase/Pck2 may function as common regulators to promote glucose or glutamine utilization toward biosynthetic pathways to promote proliferation or cell growth.[34,35] However, Pck2-mediated one-carbon signals may directly impact histone modification to influence gene expression.[45] Our study provides strong evidence that *Lin28a* is major regulator of pathological cardiac hypertrophy, which directly bound *Pck2* mRNA to facilitate the metabolic repatterning in response to cardiac stress. These results are consistent with previous findings that metabolic shift precedes ventricular hypertrophic growth,[46–48] and support the idea that metabolic repatterning during the early stage of cardiac hypertrophy could be instrumental in cardiac structural remodeling. Thus, the identification of metabolic regulators, such as Lin28a/Pck2, may provide potential therapeutic options to those who have pathological hypertrophy and heart failure.

ARTICLE INFORMATION

Received September 4, 2018; accepted November 26, 2018.

The online-only Data Supplement is available with this article at https://www.ahajournals.org/doi/suppl/10.1161/CIRCULATIONAHA.118.037803.

Correspondence

Li Qian, PhD or Jiandong Liu, PhD, Department of Pathology and Laboratory Medicine, McAllister Heart Institute, University of North Carolina at Chapel Hill, 111 Mason Farm Rd, Chapel Hill, NC 27599. Email li_qian@med.unc.edu or jiandong_liu@med.unc.edu

Affiliations

Department of Pathology and Laboratory Medicine (H.M., S.Y., Y.Z., T.F., Z.L., C.Y., J.M.T., L.Q., J.L.), and McAllister Heart Institute (H.M., S.Y., Y.Z., T.F., Z.L., C.Y., J.M.T., L.Q., J.L.), University of North Carolina at Chapel Hill. Department of Pharmacology and Cancer Biology, Duke University School of Medicine, Duke University, Durham, NC (X.L., J.W.L.). Department of Statistics, University of California at Irvine (W.S.).

Acknowledgments

We thank Dr Daley for generously sharing the *Lin28a*$^{fl/fl}$ mice line. We thank UNC Rodent Advanced Surgical Models Core, UNC High-Throughput Sequencing Facility, UNC Histology Research Core Facility, and UNC Microscopy Services Laboratory for technical support. We also thank Dr Jing Zhang in Dr Qing Zhang's laboratory and Dr Aiwen Jin in Dr Yanping Zhang's laboratory in the UNC Lineberger Comprehensive Cancer Center for help running the experiments utilizing the Seahorse Bioscience XF24 analyzer. We thank members of the Qian laboratory and the Liu laboratory for helpful discussions and critical reviews of the manuscript.

Sources of Funding

This study was supported by American Heart Association (AHA) 13SDG17060010, Ellison Medical Foundation (EMF) AG-NS-1064-13, and National Institutes of Health (NIH)/National Heart, Lung, and Blood Institute (NHLBI) R01HL128331 (to Dr Qian), NIH/ NHLBI R00 HL109079, R56HL133081, and AHA 15GRNT25530005 (to Dr Liu).

Disclosures

None.

REFERENCES

1. Frey N, Katus HA, Olson EN, Hill JA. Hypertrophy of the heart: a new therapeutic target? *Circulation*. 2004;109:1580–1589. doi: 10.1161/01.CIR.0000120390.68287.BB
2. Hill JA, Olson EN. Cardiac plasticity. *N Engl J Med*. 2008;358:1370–1380. doi: 10.1056/NEJMra072139
3. Xie M, Burchfield JS, Hill JA. Pathological ventricular remodeling: therapies: part 2 of 2. *Circulation*. 2013;128:1021–1030. doi: 10.1161/CIRCULATIONAHA.113.001879
4. Whelton PK, Carey RM, Aronow WS, Casey DE Jr, Collins KJ, Dennison Himmelfarb C, DePalma SM, Gidding S, Jamerson KA, Jones DW, MacLaughlin EJ, Muntner P, Ovbiagele B, Smith SC Jr, Spencer CC, Stafford RS, Taler SJ, Thomas RJ, Williams KA Sr, Williamson JD, Wright JT Jr. 2017 ACC/AHA/AAPA/ABC/ACPM/AGS/APhA/ASH/ASPC/NMA/PCNA Guideline for the prevention, detection, evaluation, and management of high blood pressure in adults: a report of the American College of Cardiology/American Heart Association Task Force on Clinical Practice Guidelines. *Circulation*. 2018;138:e484–e594. doi: 10.1161/CIR.0000000000000596
5. Katholi RE, Couri DM. Left ventricular hypertrophy: major risk factor in patients with hypertension: update and practical clinical applications. *Int J Hypertens*. 2011;2011:495349. doi: 10.4061/2011/495349
6. Kolwicz SC Jr, Tian R. Glucose metabolism and cardiac hypertrophy. *Cardiovasc Res*. 2011;90:194–201. doi: 10.1093/cvr/cvr071
7. Friddle CJ, Koga T, Rubin EM, Bristow J. Expression profiling reveals distinct sets of genes altered during induction and regression of cardiac hypertrophy. *Proc Natl Acad Sci USA*. 2000;97:6745–6750. doi: 10.1073/pnas.100127897
8. Heineke J, Molkentin JD. Regulation of cardiac hypertrophy by intracellular signalling pathways. *Nat Rev Mol Cell Biol*. 2006;7:589–600. doi: 10.1038/nrm1983
9. Brinegar AE, Cooper TA. Roles for RNA-binding proteins in development and disease. *Brain Res*. 2016;1647:1–8. doi: 10.1016/j.brainres.2016.02.050
10. Gerstberger S, Hafner M, Tuschl T. A census of human RNA-binding proteins. *Nat Rev Genet*. 2014;15:829–845. doi: 10.1038/nrg3813
11. Fu XD, Ares M Jr. Context-dependent control of alternative splicing by RNA-binding proteins. *Nat Rev Genet*. 2014;15:689–701. doi: 10.1038/nrg3778
12. Viswanathan SR, Daley GQ. Lin28: A microRNA regulator with a macro role. *Cell*. 2010;140:445–449. doi: 10.1016/j.cell.2010.02.007
13. Tsialikas J, Romer-Seibert J. LIN28: roles and regulation in development and beyond. *Development*. 2015;142:2397–2404. doi: 10.1242/dev.117580
14. Zhu H, Shyh-Chang N, Segrè AV, Shinoda G, Shah SP, Einhorn WS, Takeuchi A, Engreitz JM, Hagan JP, Kharas MG, Urbach A, Thornton JE, Triboulet R, Gregory RI, Altshuler D, Daley GQ; DIAGRAM Consortium; MAGIC Investigators. The Lin28/let-7 axis regulates glucose metabolism. *Cell*. 2011;147:81–94. doi: 10.1016/j.cell.2011.08.033
15. Shyh-Chang N, Zhu H, Yvanka de Soysa T, Shinoda G, Seligson MT, Tsanov KM, Nguyen L, Asara JM, Cantley LC, Daley GQ. Lin28 enhances tissue repair by reprogramming cellular metabolism. *Cell*. 2013;155:778–792. doi: 10.1016/j.cell.2013.09.059
16. Ma X, Li C, Sun L, Huang D, Li T, He X, Wu G, Yang Z, Zhong X, Song L, Gao P, Zhang H. Lin28/let-7 axis regulates aerobic glycolysis and cancer progression via PDK1. *Nat Commun*. 2014;5:5212. doi: 10.1038/ncomms6212
17. Balzer E, Moss EG. Localization of the developmental timing regulator Lin28 to mRNP complexes, P-bodies and stress granules. *RNA Biol*. 2007;4:16–25. doi: 10.4161/rna.4.1.4364
18. Chang TC, Zeitels LR, Hwang HW, Chivukula RR, Wentzel EA, Dews M, Jung J, Gao P, Dang CV, Beer MA, Thomas-Tikhonenko A, Mendell JT. Lin-28B transactivation is necessary for Myc-mediated let-7 repression and proliferation. *Proc Natl Acad Sci USA*. 2009;106:3384–3389. doi: 10.1073/pnas.0808300106
19. Dangi-Garimella S, Yun J, Eves EM, Newman M, Erkeland SJ, Hammond SM, Minn AJ, Rosner MR. Raf kinase inhibitory protein suppresses a metas-

tasis signalling cascade involving LIN28 and let-7. *EMBO J*. 2009;28:347–358. doi: 10.1038/emboj.2008.294
20. Weber KT, Brilla CG. Pathological hypertrophy and cardiac interstitium: fibrosis and renin-angiotensin-aldosterone system. *Circulation*. 1991;83:1849–1865.
21. Kong P, Christia P, Frangogiannis NG. The pathogenesis of cardiac fibrosis. *Cell Mol Life Sci*. 2014;71:549–574. doi: 10.1007/s00018-013-1349-6
22. Dobaczewski M, Chen W, Frangogiannis NG. Transforming growth factor (TGF)-β signaling in cardiac remodeling. *J Mol Cell Cardiol*. 2011;51:600–606. doi: 10.1016/j.yjmcc.2010.10.033
23. Khalil H, Kanisicak O, Prasad V, Correll RN, Fu X, Schips T, Vagnozzi RJ, Liu R, Huynh T, Lee SJ, Karch J, Molkentin JD. Fibroblast-specific TGF-β-Smad2/3 signaling underlies cardiac fibrosis. *J Clin Invest*. 2017;127:3770–3783. doi: 10.1172/JCI94753
24. Daniels A, van Bilsen M, Goldschmeding R, van der Vusse GJ, van Nieuwenhoven FA. Connective tissue growth factor and cardiac fibrosis. *Acta Physiol (Oxf)*. 2009;195:321–338. doi: 10.1111/j.1748-1716.2008.01936.x
25. Accornero F, van Berlo JH, Correll RN, Elrod JW, Sargent MA, York A, Rabinowitz JE, Leask A, Molkentin JD. Genetic analysis of connective tissue growth factor as an effector of transforming growth factor β signaling and cardiac remodeling. *Mol Cell Biol*. 2015;35:2154–2164. doi: 10.1128/MCB.00199-15
26. Viswanathan SR, Daley GQ, Gregory RI. Selective blockade of microRNA processing by Lin28. *Science*. 2008;320:97–100. doi: 10.1126/science.1154040
27. Heo I, Joo C, Cho J, Ha M, Han J, Kim VN. Lin28 mediates the terminal uridylation of let-7 precursor MicroRNA. *Mol Cell*. 2008;32:276–284. doi: 10.1016/j.molcel.2008.09.014
28. Yang Y, Ago T, Zhai P, Abdellatif M, Sadoshima J. Thioredoxin 1 negatively regulates angiotensin II-induced cardiac hypertrophy through upregulation of miR-98/let-7. *Circ Res*. 2011;108:305–313. doi: 10.1161/CIRCRESAHA.110.228437
29. Polesskaya A, Cuvellier S, Naguibneva I, Duquet A, Moss EG, Harel-Bellan A. Lin-28 binds IGF-2 mRNA and participates in skeletal myogenesis by increasing translation efficiency. *Genes Dev*. 2007;21:1125–1138. doi: 10.1101/gad.415007
30. Balzer E, Heine C, Jiang Q, Lee VM, Moss EG. LIN28 alters cell fate succession and acts independently of the let-7 microRNA during neurogliogenesis *in vitro*. *Development*. 2010;137:891–900. doi: 10.1242/dev.042895
31. Hafner M, Max KE, Bandaru P, Morozov P, Gerstberger S, Brown M, Molina H, Tuschl T. Identification of mRNAs bound and regulated by human LIN28 proteins and molecular requirements for RNA recognition. *RNA*. 2013;19:613–626. doi: 10.1261/rna.036491.112
32. Cho J, Chang H, Kwon SC, Kim B, Kim Y, Choe J, Ha M, Kim YK, Kim VN. LIN28A is a suppressor of ER-associated translation in embryonic stem cells. *Cell*. 2012;151:765–777. doi: 10.1016/j.cell.2012.10.019
33. Liu X, Romero IL, Litchfield LM, Lengyel E, Locasale JW. Metformin targets central carbon metabolism and reveals mitochondrial requirements in human cancers. *Cell Metab*. 2016;24:728–739. doi: 10.1016/j.cmet.2016.09.005
34. Brown DM, Williams H, Ryan KJ, Wilson TL, Daniel ZC, Mareko MH, Emes RD, Harris DW, Jones S, Wattis JA, Dryden IL, Hodgman TC, Brameld JM, Parr T. Mitochondrial phosphoenolpyruvate carboxykinase (PEPCK-M) and serine biosynthetic pathway genes are co-ordinately increased during anabolic agent-induced skeletal muscle growth. *Sci Rep*. 2016;6:28693. doi: 10.1038/srep28693
35. Montal ED, Dewi R, Bhalla K, Ou L, Hwang BJ, Ropell AE, Gordon C, Liu WJ, DeBerardinis RJ, Sudderth J, Twaddel W, Boros LG, Shroyer KR, Duraisamy S, Drapkin R, Powers RS, Rohde JM, Boxer MB, Wong KK, Girnun GD. PEPCK coordinates the regulation of central carbon metabolism to promote cancer cell growth. *Mol Cell*. 2015;60:571–583. doi: 10.1016/j.molcel.2015.09.025
36. Ferrans VJ, Jones M, Maron BJ, Roberts WC. The nuclear membranes in hypertrophied human cardiac muscle cells. *Am J Pathol*. 1975;78:427–460.
37. Ye J, Mancuso A, Tong X, Ward PS, Fan J, Rabinowitz JD, Thompson CB. Pyruvate kinase M2 promotes de novo serine synthesis to sustain mTORC1 activity and cell proliferation. *Proc Natl Acad Sci USA*. 2012;109:6904–6909. doi: 10.1073/pnas.1204176109
38. Ducker GS, Rabinowitz JD. One-carbon metabolism in health and disease. *Cell Metab*. 2017;25:27–42. doi: 10.1016/j.cmet.2016.08.009
39. Tsanov KM, Pearson DS, Wu Z, Han A, Triboulet R, Seligson MT, Powers JT, Osborne JK, Kane S, Gygi SP, Gregory RI, Daley GQ. LIN28 phosphorylation by MAPK/ERK couples signalling to the post-transcriptional control of pluripotency. *Nat Cell Biol*. 2017;19:60–67. doi: 10.1038/ncb3453
40. Piskounova E, Polytarchou C, Thornton JE, LaPierre RJ, Pothoulakis C, Hagan JP, Iliopoulos D, Gregory RI. Lin28A and Lin28B inhibit let-7 microRNA biogenesis by distinct mechanisms. *Cell*. 2011;147:1066–1079. doi: 10.1016/j.cell.2011.10.039
41. Izumo S, Nadal-Ginard B, Mahdavi V. Protooncogene induction and reprogramming of cardiac gene expression produced by pressure overload. *Proc Natl Acad Sci USA*. 1988;85:339–343. doi: 10.1073/pnas.85.2.339
42. Park JY, Li W, Zheng D, Zhai P, Zhao Y, Matsuda T, Vatner SF, Sadoshima J, Tian B. Comparative analysis of mRNA isoform expression in cardiac hypertrophy and development reveals multiple post-transcriptional regulatory modules. *PLoS One*. 2011;6:e22391. doi: 10.1371/journal.pone.0022391
43. Fernández-Ruiz I. Growth and development: poly(A) tail-based regulation of cardiac hypertrophy. *Nat Rev Cardiol*. 2017;14:504. doi: 10.1038/nrcardio.2017.113
44. Buchan JR, Parker R. Eukaryotic stress granules: the ins and outs of translation. *Mol Cell*. 2009;36:932–941. doi: 10.1016/j.molcel.2009.11.020
45. Zhang J, Ratanasirintrawoot S, Chandrasekaran S, Wu Z, Ficarro SB, Yu C, Ross CA, Cacchiarelli D, Xia Q, Seligson M, Shinoda G, Xie W, Cahan P, Wang L, Ng SC, Tintara S, Trapnell C, Onder T, Loh YH, Mikkelsen T, Sliz P, Teitell MA, Asara JM, Marto JA, Li H, Collins JJ, Daley GQ. LIN28 regulates stem cell metabolism and conversion to primed pluripotency. *Cell Stem Cell*. 2016;19:66–80. doi: 10.1016/j.stem.2016.05.009
46. Doenst T, Pytel G, Schrepper A, Amorim P, Färber G, Shingu Y, Mohr FW, Schwarzer M. Decreased rates of substrate oxidation ex vivo predict the onset of heart failure and contractile dysfunction in rats with pressure overload. *Cardiovasc Res*. 2010;86:461–470. doi: 10.1093/cvr/cvp414
47. Zhang L, Jaswal JS, Ussher JR, Sankaralingam S, Wagg C, Zaugg M, Lopaschuk GD. Cardiac insulin-resistance and decreased mitochondrial energy production precede the development of systolic heart failure after pressure-overload hypertrophy. *Circ Heart Fail*. 2013;6:1039–1048. doi: 10.1161/CIRCHEARTFAILURE.112.000228
48. Czarnowska E, Bierła JB, Toczek M, Tyrankiewicz U, Pająk B, Domal-Kwiatkowska D, Ratajska A, Smoleński RT, Mende U, Chłopicki S. Narrow time window of metabolic changes associated with transition to overt heart failure in Tgaq*44 mice. *Pharmacol Rep*. 2016;68:707–714. doi: 10.1016/j.pharep.2016.03.013